Weak Hypoxia Enhanced Denitrification in a Dissimilatory Nitrate Reduction to Ammonium (DNRA)-Dominated Shallow and Eutrophic Coastal Waterbody, Jinhae Bay, South Korea

Yan Huang and Soonmo An [*]

Department of Oceanography, College of Natural Sciences, Pusan National University, Busan, South Korea

The effects of seasonal hypoxia on sediment-water interface nitrogen (N) transformations in Jinhae Bay were examined from 2015 to 2019. The rates of benthic denitrification, anaerobic ammonium oxidation (anammox), dissimilatory nitrate reduction to ammonium (DNRA), nutrient exchange, and sediment oxygen consumption were measured seasonally. The oxygen (O_2) and hydrogen sulfide (H_2S) depth profiles were measured using microelectrodes. Neither penetration nor consumption of oxygen decreased during hypoxia. Denitrification, anammox, and DNRA ranged from 0 to 0.73, 0.13, and 1.09 mmol N m^{-2} day^{-1}, respectively. Denitrification, the dominant N removal pathway, increased by 75% while anammox ceased, which led to an overall increase of 55% in the total N_2 gas production during hypoxia relative to that during normoxia. Enhanced denitrification is the result of increased coupled nitrification–denitrification due to the intermittent supply of oxygen during bottom water hypoxia ("weak hypoxia"). In the hypoxic period, DNRA decreased by 62%, and the relative contribution of DNRA to the total nitrogen reduction process decreased from 81 to 58%, but it still outperformed denitrification as the main nitrate reduction pathway. Sediments were strong sources of ammonium for the water column, both under normoxia and hypoxia, whereas they were a sink of nitrate from the water column during hypoxia. Bioturbation may be important for maintaining oxygen penetration and consumption in sediments. The dominance of DNRA was mainly due to the relatively high content of sulfide and organic-rich sediments. The repressed macrofaunal activity and increased coupling of nitrification and denitrification during hypoxia may have contributed to enhanced denitrification. Taken together, the overall dominance of DNRA might contribute to the development and maintenance of eutrophication and seasonal hypoxia in this system. However, in contrast to the previous results, denitrification was enhanced during "weak hypoxia," which might be helpful in alleviating eutrophication.

Keywords: weak hypoxia, denitrification, nitrification, anammox, dissimilatory nitrate reduction to ammonium, Jinhae Bay

INTRODUCTION

In the past few decades, the most important change in marine ecosystems has been the decrease in oxygen levels, both in the open ocean and coastal environments (Breitburg et al., 2018). Hypoxia occurs when the oxygen level is less than 2 ml L^{-1} or 90 µmoL L^{-1}, which suppresses macrofaunal activity and alters the biogeochemical cycling of important nutrients, such as dissolved inorganic nitrogen (Diaz and Rosenberg, 1995; Diaz and Rosenberg, 2008). In the open ocean, global warming is considered the primary cause of hypoxia, as it directly reduces the solubility of oxygen and further reduces the introduction of oxygen by increasing seawater stratification and weakening ocean overturning circulation (Helm et al., 2011; Schmidtko et al., 2017). In estuaries and coastal systems, hypoxia is mainly attributed to increased loading of nutrients (primarily N and P) and organic matter from agriculture (Hasler, 1969), sewage (Galton, 1884), and the combustion of fossil fuels in areas such as the Mississippi River-influenced Gulf of Mexico (Rabalais et al., 2007), East China Sea (Tong and Zhang, 2007; Wei et al., 2007), and Chesapeake Bay (Kemp et al., 2005; Kemp et al., 2009; Rabalais et al., 2010).

In most cases, hypoxia is particularly evident in semi-enclosed coastal waters where water exchange is poor. Jinhae Bay, the largest semi-enclosed bay in South Korea, is located on the south-eastern coast. It suffers frequent bottom-water hypoxic events and has been reported as one of the "Korean dead zones" (Lee et al., 2018). However, hypoxia in Jinhae Bay, which we defined as "weak hypoxia" in the current study, is temporally unstable due to the shallow water depth (see discussion). Hypoxia in Jinhae Bay is mainly caused by eutrophication due to excessive nitrogen nutrient input from human activities (Diaz and Rosenberg, 1995; Diaz and Rosenberg, 2008). Approximately, 7.5% of the sea area of Jinhae Bay is used for aquaculture, including production of oysters, mussels, and ark shells (Kim et al., 2013); it is the largest shellfish production area in Korean coastal waters (Yoon et al., 2019). Since the 1960s, large amounts of untreated domestic sewage and industrial waste have been discharged into Jinhae Bay, worsening the deterioration of water quality caused by aquaculture.

Relatively few denitrifying organisms occur in the water column, whereas they are widely distributed in marine sediments, forming hotspots of nitrogen cycling that are responsible for 60% of marine fixed nitrogen loss (Eugster and Gruber, 2012). Nitrogen reduction processes are sometimes referred to as nitrogen sinks and links; these are both restricted to the anoxic part of sediments. Nitrogen sinks include denitrification and anaerobic ammonium oxidation (anammox), and the links include the dissimilatory nitrate reduction to ammonium (DNRA) process (An and Gardner, 2002). Both denitrification (often coupled with nitrification) and anammox can remove fixed nitrogen (nitrate or ammonium) from the system as nitrogen gas and reduce the reactive nitrogen. DNRA converts nitrate to ammonium, recycles it, and retains the transformed nitrogen in a biologically available form, thereby aggravating eutrophication and/or hypoxia (Deng et al., 2015).

Benthic nitrogen cycling (mainly including nitrogen fixation, nitrification, anammox, denitrification, and DNRA), especially nitrate reduction, is regulated by a variety of environmental parameters, such as substrate (nitrate) availability, dissolved oxygen concentration, organic matter content, and the presence of inhibitors (e.g., sulfide) (An and Joye, 2001; Bae et al., 2001; Jensen et al., 2008). Because benthic nitrogen cycling is closely related to oxygen conditions, a range of studies have investigated the response of sediment nitrogen cycling to bottom water oxygen availability (Neubacher et al., 2011; Jäntti and Hietanen, 2012; Neubacher et al., 2012; Bonaglia et al., 2014; McCarthy et al., 2015; Caffrey et al., 2019; Foster and Fulweiler, 2019; Song et al., 2020); however, the effect of O_2 on nitrogen cycling varies. For example, Neubacher et al. (2011; 2012) found denitrification increased under both short- and long-duration experimentally induced hypoxic conditions, whereas Song et al. (2020) found benthic N loss decreased by 38% under artificially induced severe hypoxic conditions. McCarthy et al. (2015) found that denitrification was negatively correlated with bottom water dissolved oxygen (DO) and the highest denitrification rate under the lowest ambient bottom water DO. Caffrey et al. (2019) also obtained the highest denitrification rate under hypoxic treatment, whereas Jäntti and Hietanen (2012) found that DNRA dominated nitrate reduction when $O_2 < 110$ µmol L^{-1}, and most nitrogen was recycled instead of being removed by forming N_2 gas. Foster and Fulweiler (2019) argued that there is little to no change in denitrification under hypoxic conditions. In addition, as the important nitrogen removal pathway in the nitrate reduction process, denitrification is also influenced by other factors. Rysgaard et al. (2004) suggested that denitrification is a temperature-dependent process, while Deng et al. (2015) reported a positive relationship between denitrification rates and the organic carbon contents.

Some of these studies used experimentally induced hypoxic conditions (Neubacher et al., 2011; Neubacher et al., 2012; Song et al., 2020), which makes it difficult to simulate the effects of ambient hypoxia on benthic nitrogen cycling; furthermore, these studies were generally short in duration and may not have had a temporal resolution high enough to capture the seasonal variability of potentially regulating factors (Hietanen and Lukkari, 2007). Most of these studies have focused on estuarine or coastal marine sediments, and few have focused on semi-enclosed shallow bays. Jinhae Bay is an appropriate representative field site to study the effects of seasonal bottom water hypoxia on benthic nitrogen cycling in a semi-closed bay, as these conditions regularly occur there.

In this study, we investigated how benthic nitrogen cycling responded to different bottom water oxygen levels under natural seasonal oxygen-deficient conditions *via* intact core and slurry incubations. We examined the impact of Jinhae Bay seasonal bottom water oxygen concentrations on (1) water column O_2 and nutrient dynamics; (2) benthic nitrogen reduction processes, denitrification, anammox, and DNRA; (3) benthic nitrogen transform fluxes and sediment oxygen consumption (SOC); and (4) oxygen (O_2) and hydrogen sulfide (H_2S) depth profiles.

MATERIALS AND METHODS

Sampling Site Description and Protocol

Jinhae Bay is a typical shallow bay with a water depth of less than 20 m and an approximate area of 640 km^2 (Kwon et al., 2020) (**Figure 1**), including seven small semi-enclosed inner bays (Jindong, Danghang, Dangdong, Wonmun, Gohyeon, Haengam, and Masan Bays) (Lee et al., 2018). The annual precipitation is approximately 1,500 mm, concentrated in the summer months, and the air temperature ranges from -5°C to 35°C. Jinhae Bay is dominated by semidiurnal tides, with a high current speed at the mouth of the bay and less than 10 cm s^{-1}, current speed within the inner bay (Kim et al., 2015). Water exchange in the inner bay is poor and minimally affected by freshwater discharge. Hypoxia has been reported every summer since 1974 due to water column stratification (Cho et al., 2002).

Sampling and experiments were conducted at several sites in Jinhae Bay over 16 cruises from 2015 to 2019 (**Figure 1**). Dangdong Bay (DD), Danghang Bay (DH), and Wonmun Bay (WM) were selected to examine benthic nitrogen cycling and oxygen dynamics over the course of five years. Because hypoxia occurred more frequently and severely (based on our previous study) than in the other two sites (DH and WM), two stations (DD1 and DD2) were selected in Dangdong Bay. The details of the sites visited during each cruise are listed in **Table 1**.

Depth profiles of temperature, salinity, and DO were acquired using a HydroLab multiprobe system (HydroLab ® 4a) system. Water column samples for nutrient analysis were collected at the surface (0–0.5 m), middle (4.5–8 m, based on different water depths of each station), and bottom (0.5 m above sediment). Samples for nutrient analysis were filtered immediately upon collection through GF/F glass fiber syringe filters (Whatman International, Maidstone, Kent, UK) and transferred into 50 mL sterile centrifugal tubes (Thermo Fisher Scientific, US). Bottom water samples were collected in a 5 L Niskin bottle for subsequent incubation experiments. Small (internal diameter (ID) 4 cm; height 23 cm) and large (ID 8 cm; height 33 cm) intact sediment cores and overlying water were collected with acrylic corers by scuba divers with minimal disturbance to the sediment–water interface (An and Joye, 2001). The sediment cores and water samples were sealed with polyvinyl chloride (PVC) caps immediately after collection and transferred to the laboratory within 2 or 3 h. The sediments were mainly composed of fine-grained silty clays and clays with high organic matter content, of which the organic carbon content was the highest amongst those of all Korean coastal sediments (Seo et al., 2015). Macrofaunal burrows were observed in the sediment cores. Unamended intact core incubation data were available from January (Jan) 2015 to March (Mar) 2017 (**Table 2**), whereas slurry incubation and DNRA data were available from July (Jul) 2016 to November (Nov) 2019.

Water Column and Sediment Profiles

We immediately stored the water column samples in a -20°C freezer until nutrient analysis. Dissolved inorganic ammonium (NH_4^+), nitrate (NO_3^-), and nitrite (NO_2^-) (i.e., NOx)
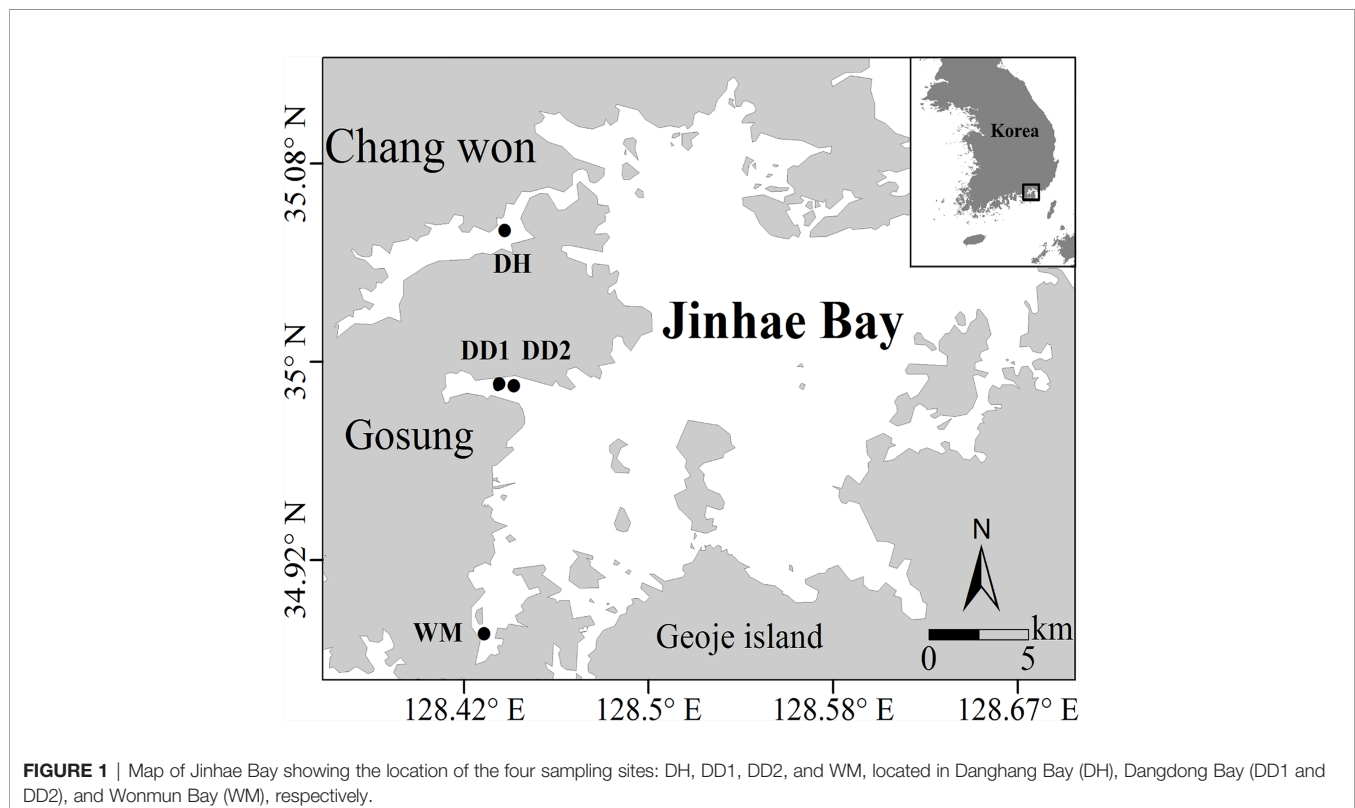
FIGURE 1 | Map of Jinhae Bay showing the location of the four sampling sites: DH, DD1, DD2, and WM, located in Danghang Bay (DH), Dangdong Bay (DD1 and DD2), and Wonmun Bay (WM), respectively.

TABLE 1 | Ambient bottom water (approximately 0.5 m above sediment surface) conditions at sites sampled on cruises in Jinhae Bay.

Site ID	Cruise	Depth (m)	Temperature (°C)	Salinity (psu)	DO ($\mu mol\ L^{-1}$)	NOx ($\mu mol\ L^{-1}$)	NH$_4$
DH	Jan 2015	14	6.4	31.1	289.4	1.2	1.3
	Apr 2015	13.2	12.4	31	252.2	4.6	2.6
	May 2015	13.2	14.3	30.5	266.6	3.6	1.3
	Jun 2015	14.3	18.3	33.8	112.6	5.5	4.6
	Jul 2015	14.1	21.7	30.8	55.6[a]	6.4	8.5
	Sep 2015	13.9	24.6	29.8	90.3[a]	4.0	7.2
	Oct 2015	14	20.8	30.9	153.1	4.9	4.6
	Nov 2015	14.2	14.9	30.5	261.9	11.8	3.7
WM	Jan 2015	12.8	6.2	31.3	299.1	3.0	1.6
	Apr 2015	9	12.3	31.3	247.2	2.6	0.9
	May 2015	9.5	13.3	31.3	195.6	2.2	1.0
	Jun 2015	9.8	15.7	33.9	42.6][a]	2.1	6.6
	Jul 2015	9.8	21.6	31.2	118.8	8.8	1.8
	Sep 2015	9.2	25.0	30.1	185.3	2.1	0.6
	Oct 2015	9.2	21.4	30.9	144.1	0.9	3.1
	Nov 2015	10.1	14.8	31.1	204.1	7.5	5.4
	Jul 2016	9.3	19.4	31.7	23.1[a]	0.9	0.8
	Aug 2016	9.7	26.4	31.1	95.6	1.1	6.0
DD1	Jan 2015	12.8	6.1	31.4	304.4	4.5	1.1
	Apr 2015	13	11.7	31.6	247.8	2.0	0.8
	May 2015	13.9	12.4	31.4	228.1	2.3	0.8
	Jun 2015	16	15.3	34.5	10.6[a]	2.9	20.3
	Jul 2015	16.3	20.1	31.7	4.7[a]	6.6	3.3
	Sep 2015	16.8	24.5	30.4	90[a]	2.6	6.1
	Oct 2015	16	21	31.3	51.9[a]	5.1	8.5
	Nov 2015	17.3	15.1	31.6	211.9	5.6	3.9
	Jul 2016	15.5	17.4	32.3	30.9[a]	15.7	2.1
	Aug 2016	15.8	22.6	31.1	61.9[a]	1.5	9.4
	Mar 2017	15.8	8.7	33.1	260.3	1.1	1.4
DD2	Jul 2016	14.7	17.5	32.3	17.8[a]	14.1	4.3
	Aug 2016	15.6	21.7	31.2	13.8[a]	0.9	9.9
	Mar 2017	15.6	9	33.1	274.7	1.1	0.7
	Dec 2018	15.3	12.7	32.8	306.3	–	–
	Apr 2019	15	12.8	29.5	243.8	1.1	2.3
	May 2019	15.2	15.1	27.5	164.4	1.5	5.7
	Aug 2019	14.7	20.8	35	53.1[a]	1.3	7.1
	Nov 2019	13.9	15.9	32.6	244.7	6.1	1.5

DO, dissolved oxygen; NOx, nitrate plus nitrite; NH_4^+, ammonium.
[a]Bottom water hypoxia (DO < 90 $\mu mol\ L^{-1}$).

concentrations in the filtered ambient and core incubation samples were determined by standard methods using a spectrophotometer (Shimadzu, UV-1650PC, Japan) (Strickland and Parsons, 1972). Ammonium-free seawater with similar salinity was used to prepare standard solution to eliminate the influence of salinity on the determination of ammonium (NH_4^+) (Parsons et al., 1984). Sediment characteristics, including water content (%), grain size >63 μm (sand content, %), and sediment organic matter content (loss-on-ignition (LOI) %), were measured using a large intact core. The sediment core was sliced at intervals of 1 cm within the first 10 cm and at intervals of 2 cm above 10 cm. The water content was measured by the weight loss of the sediment after drying in an oven at 60°C for 24 h. Grain size >63 μm was determined using a copper sieve (230 mesh, 63 μm). Sediment organic matter content, expressed as the percentage of weight loss-on-ignition (LOI %), was calculated after combustion at 550°C for 2 h. The microprofiles of dissolved oxygen (O_2) and hydrogen sulfide

(H_2S) were measured during several cruises in an intact core (ID: 8 cm; height: 33 cm) using O_2 and H_2S microelectrodes (OX-50, H_2S-100, Unisense [®], Denmark).

Unamended Intact Core Incubations for Sediment Oxygen Consumption and Nutrient Flux

Six intact cores (the upper cap was removed) and in-situ bottom water (approximately 20 L) were placed in an incubation tank and pre-incubated overnight in the dark at the in-situ water temperature with O_2 saturation. The top parts of the core were sealed with a rubber stopper and immediately preincubated, and the sediment cores were incubated for approximately 24 h. Duplicate cores were sacrificed at time points of 0, 1, 2, and 24 h, and the oxygen concentration was directly determined using a membrane inlet mass spectrometer (MIMS) (Kana et al., 1994; Deng et al., 2015). Water samples for nutrient flux analysis at each time point were filtered and preserved, as described above.

TABLE 2 | Sediment–water interface sediment oxygen consumption, nutrient flux (mmol N m^{-2} day^{-1}), and nitrification in unamended cores from sites sampled in Jinhae Bay.

Site ID	Cruise	SOC	NOx-f	NH$_4$-f	Nit*
DH	15-Jan	15.5 (4.7)	0.03 (0.1)	0.56 (0.2)	0.05 (0.1)
	Apr-15	12.8 (7.5)	-0.03 (0.2)	-0.79 (0.2)	0.25 (0.1)
	May-15	13.6 (2.1)	0.26 (0.01)	-0.01 (0.3)	0.54 (0.03)
	Jun-15	13.7 (2.7)	0.15 (0.1)	-0.16 (0.2)	0.45 (0.1)
	Jul-15	17.6 (1.2)	0.42 (0.1)	-0.41 (1)	0.68 (0.04)
	Sep-15	27.2 (0.4)	-1.15 (0.1)	1.32 (1)	0 (0)
	Oct-15	21.0 (3.0)	-0.19 (0.01)	1.21 (1.9)	0.12 (0.1)
	Nov-15	8.2 (1.7)	-0.05 (0.1)	0.17 (0.8)	0.74 (0.3)
WM	Apr-15	17.3 (0.7)	0.01 (0.1)	0.37 (0.3)	0.03 (0.03)
	May-15	13.8 (3.4)	0 (0.1)	0.55 (0.1)	0.07 (0.1)
	Jun-15	23.5 (4.7)	0.14 (0.1)	1.54 (0)	0.46 (0.2)
	Jul-15	18.0 (3.3)	-0.05 (0.01)	1.49 (0.2)	0 (0)
	Sep-15	19.3 (0.8)	-0.12 (0.1)	1.51 (0)	0.03 (0.03)
	Oct-15	18.2 (0.7)	0.04 (0)	0.29 (0.3)	0.08 (0.01)
	Nov-15	8.3 (3.3)	0.15 (0.1)	0.13 (0.1)	0.31 (0.1)
	Jul-16	8.8 (0.2)	-0.05 (0.1)	0.71 (0.2)	0.01 (0.01)
	Aug-16	27.2 (0.1)	-0.1 (0.1)	0.09 (0.1)	0.17 (0.2)
DD1	Jan-15	10.6 (1.4)	0.01 (0.02)	0.2 (0.5)	0.01 (0.01)
	Apr-15	18.1 (4.7)	-0.09 (0.03)	1.2 (0.8)	0 (0)
	May-15	13.2 (6.2)	0.18 (0.2)	0.23 (1.1)	0.28 (0.2)
	Jun-15	14.7 (2.0)	0.03 (0.3)	-0.4 (0.4)	0.44 (0.3)
	Jul-15	19.6 (2.0)	0.09 (0.2)	0.97 (0.3)	0.17 (0.2)
	Sep-15	27.3 (2.4)	-0.17 (0.1)	0.66 (0.1)	0.06 (0.1)
	Oct-15	19.5 (1.7)	-0.13 (0)	0.55 (0.3)	0.03 (0.03)
	Nov-15	14.3 (0.7)	-0.27 (0.04)	2.49 (0.7)	0 (0)
	Jul-16	7.4 (1.2)	-0.07 (0.1)	-0.35 (0.1)	0.04 (0.04)
	Aug-16	20.3 (0.2)	-0.07 (0.01)	-0.43 (0.1)	0.02 (0.02)
	Mar-17	15.3 (2.5)	-0.02 (0)	0.2 (0)	0 (0)
DD2	Jul-16	22.0 (5.7)	-0.78 (0)	0.91 (0.9)	0 (0)
	Aug-16	25.8 (0.5)	0.06 (0.03)	-0.35 (0.1)	0.52 (0.03)
	Mar-17	12.1 (2.7)	0.1 (0.01)	-0.2 (0.2)	0.1 (0.01)

f, flux; SOC, sediment oxygen consumption; Nit, nitrification.

Note the values in parentheses represent the standard error of rates measured in duplicate samples (values less than 0.05 are accurate to two decimal places to distinguish them from true zeros).

*Nitrification was estimated by the approach of Neubacher et al. (2011).

Slurry and Amended Intact Core Incubations for Benthic Denitrification, Anammox, and DNRA

Slurry incubations were conducted to determine the potential denitrification, anammox, and DNRA rates and their relative contributions to the total nitrate reduction process according to Thamdrup and Dalsgaard (2002) and Shan et al. (2016). Briefly, the sectioned subsamples (0–3 cm) were sieved through a 1.0 mm copper sieve to remove visible shells or roots prior to subsequent analysis (Wang et al., 2020). Then, 3 mL of sediment and He-purged bottom water were transferred to 40 mL gas-tight glass vials (Exetainer, Labco, UK) and sealed immediately to avoid bubbles or any headspace. The slurries were preincubated overnight to consume residual O$_2$ and NOx and then received one of three different tracer combinations (^{15}NH$_4$Cl, ^{15}NH$_4$Cl plus K^{14}NO$_3$, or Na^{15}NO$_3$, 98–99% atom %, Sigma-Aldrich) to a final concentration of approximately 100 µmol L^{-1} ^{15}N in each vial. The bottle was vigorously shaken after the addition of the tracer so that the ^{15}N was evenly distributed in the slurry. After 18–24 h when the ^{15}N tracer reached a new equilibrium state, triplicate vials were sacrificed at time points of 0, 24, 48, and 72 h. Nitrogen gas (^{29}N$_2$, ^{30}N$_2$) production was

analyzed immediately, as described above. The ^{15}NO$_3^-$ amended slurry samples were also used for ^{15}NH$_4^+$ analysis.

^{15}NO$_3^-$ amended intact core incubations were performed to determine the benthic denitrification, anammox, and DNRA rates. The incubation tank was amended with the ^{15}NO$_3^-$ tracer (Na^{15}NO$_3$, 98% ^{15}N atom %, Sigma) to a final concentration of 100 µmol L^{-1}. The sediment cores were then preincubated overnight to allow the stabilization and equilibration of NO$_3^-$. The following day, the nitrogen gas produced during the incubation (^{29}N$_2$, ^{30}N$_2$) in duplicate cores was directly determined using a MIMS at time points of 0, 1, 2, and 24 h. Time series samples for ^{15}NH$_4^+$ analysis were also collected simultaneously. DNRA activity was measured using the OX/MIMS method (^{15}NH$_4^+$ oxidation technique and MIMS analysis) according to Yin et al. (2014). Briefly, all ^{15}NH$_4^+$ samples were purged with He gas to eliminate any ^{29}N$_2$ and ^{30}N$_2$ produced by denitrification and/or anammox during intact core/slurry incubations. The He-purged samples were transferred to 12 mL gas-tight glass vials, and hypobromite iodine solution (0.2 mL) was added to oxidize any ^{15}NH$_4^+$ into ^{15}N gases (^{29}N$_2$ and ^{30}N$_2$). The production of nitrogen gas (^{29}N$_2$, ^{30}N$_2$) was analyzed using a MIMS and used to calculate the DNRA rates.

Rate Calculation

The slope of the linear regression of the measured O_2, $^{29}N_2$, and $^{29}N_2$ and nutrient concentrations against time was used to calculate the rate. The units for sediment oxygen uptake ($\mu mol\ O_2\ L^{-1}\ h^{-1}$) and nutrient flux ($\mu mol\ N\ L^{-1}\ h^{-1}$) and rates of benthic nitrogen reduction processes (denitrification, anammox, and DNRA, $\mu mol\ N\ L^{-1}\ h^{-1}$) in the core incubation were converted to $mmol\ O_2\ m^{-2}\ d^{-1}$ and $mmol\ N\ m^{-2}\ d^{-1}$, respectively, by dividing by the intact incubation sediment surface area.

Anammox activity was confirmed by $^{15}NH_4^+$ tracer-amended anoxic slurry incubation (Thamdrup and Dalsgaard, 2002). Therefore, N_2 production was derived from both denitrification and anammox in intact core incubations, from which the actual denitrification and anammox rates were calculated according to the revised isotope pairing technique (r-IPT) (Risgaard-Petersen et al., 2003). Briefly, the total N_2 production (P_{14}) was expressed as a function of r_{14}, which is the ratio of $^{14}NO_3^-$ to $^{15}NO_3^-$ in the nitrate reduction process.

$$P_{14} = 2 \times r_{14} \times \left[P^{29}N_2 + P^{30}N_2 \times (1 - r_{14}) \right] \quad (1)$$

where $P^{29}N_2$ and $P^{30}N_2$ are the production rates of $^{29}N_2$ and $^{30}N_2$, respectively, calculated from the linear regression of the measured concentration against time. Parameter r_{14} can be derived from anoxic slurry incubation as follows:

$$r_{14} = \left[(1 - ra) \times R_{29} - ra \right] / (2 - ra) \quad (2)$$

where ra is the anammox contribution to the total N_2 production in the anoxic slurry incubation and R_{29} is the ratio of $P^{29}N_2$ to $P^{30}N_2$ derived during core incubation; however, we used the estimated ra by averaging the measured value of ra in the normoxia and hypoxia periods, when anoxic slurry incubation was not conducted.

The genuine anammox (aao_{14}) and denitrification (den_{14}) rates in the core incubation were calculated using the following formulae:

$$aao_{14} = 2 \times r_{14} \times (P^{29}N_2 - 2 \times r_{14} \times P^{30}N_2) \quad (3)$$

$$den_{14} = P_{14} - aao_{14} \quad (4)$$

The proportion of P_{14} supported by $^{14}NO_3^-$ from the water column ($P_{14}w$) was calculated as follows:

$$P_{14}w = P_{14} \times f_{14} / r_{14} \quad (5)$$

where f_{14} represents the ratio between the concentrations of $^{14}NO_3^-$ and $^{15}NO_3^-$ in the water column from the intact core incubation.

The proportion of P_{14} supported by sedimentary nitrification ($P14n$) was calculated as follows:

$$P_{14}n = P_{14} - P_{14w} \quad (6)$$

We estimated nitrification rates according to Neubacher et al. (2011).

Statistical Analyses

All statistical analyses were performed using Statistical Package for the Social Sciences (SPSS) version 22. One-way analysis of variance (ANOVA) was used to test for differences between seasons and sites. We conducted a Pearson correlation analysis to evaluate the correlations among SOC, N transformation rates (nutrient flux, denitrification, anammox, and DNRA), and environmental parameters.

RESULTS

Sampling Site Water Column and Sediment Physicochemical Characteristics

The physicochemical characteristics of the sites are summarized in **Table 1**. The water depth at sampling sites varied between 9 and 17.3 m. Surface water and bottom water temperatures varied between 6 and 29.9°C and 6.1 and 26.4°C, respectively. The temperature peaked in the summer and decreased in the winter. Salinity ranged between 25 and 33.7 and 27.5 and 35 psu for surface and bottom water, respectively. No significant spatial or seasonal variations in the salinity were observed. Surface and bottom water DO ranged from 155.3–408.1 $\mu mol\ L^{-1}$ and 4.7–306.3 $\mu mol\ L^{-1}$, respectively. Both values were high at the DH site and low at the DD site. A significant seasonal variation in DO was observed; DO was low in summer and autumn and high in winter and spring (one-way ANOVA, n = 37, P = 0.000). Bottom water hypoxia ($O_2 < 90\ \mu mol\ L^{-1}$) occurred at all stations during the sampling periods in summer and autumn. The lowest bottom water O_2 concentration, 4.7 $\mu mol\ L^{-1}$, was recorded at DD1 station in Jul 2015.

An obvious spatial variation was observed between water column NOx (one-way ANOVA, n = 108, P = 0.004), with the highest concentration of 5.7 $\mu mol\ L^{-1}$ recorded at DH station, the median value of 3.3 $\mu mol\ L^{-1}$ at DD1 station, and the lowest two values (2.9 and 2.6 $\mu mol\ L^{-1}$) at WM and DD2 stations (data not shown). Seasonal variations were observed in the water column NH_4^+ concentrations (n = 108, P = 0.014). Generally, water column nutrient concentrations were high in summer and autumn (hypoxia period) and low in spring and winter (normoxic period) (**Table 1**). The water column dissolved inorganic N (DIN = NOx+NH_4^+) concentrations averaged 6.4 ± 0.5 $\mu mol\ L^{-1}$, which were much higher in bottom water in autumn (8.2 ± 0.9 $\mu mol\ L^{-1}$) and summer (6.9 ± 0.8 $\mu mol\ L^{-1}$) than in spring (4.7 ± 0.6 $\mu mol\ L^{-1}$) and winter (3.7 ± 0.4 $\mu mol\ L^{-1}$).

The water content of surface sediment (0–3 cm) ranged from 62% to 80% (data not shown). The organic matter content of the surface sediment was the highest in summer (18%), followed by spring (17%) and autumn (15%), and the lowest in winter (12%). Overall, the sediments were fine-grained and rich in organic matter (OM).
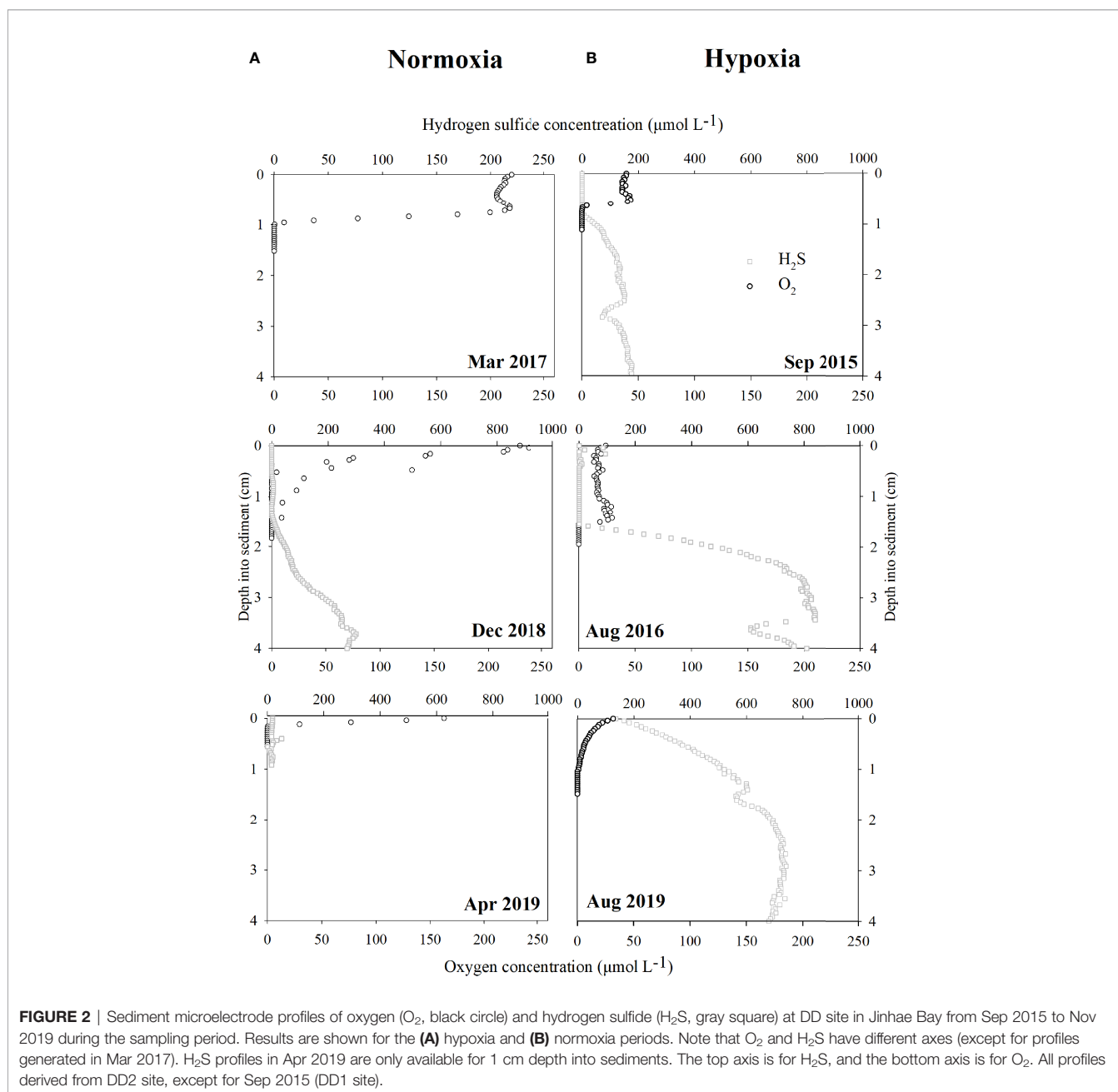
Oxygen and H$_2$S Microelectrode Profiles

Sediment O_2 and H_2S profiles were generated by duplicate microelectrode measurements in one core from each site during

several cruises from September (Sep) 2015 to Nov 2019. A complete seasonal profile was only available for Dangdong Bay (**Figure 2**). The concentration of pore water oxygen fluctuated, with no clear and stable decreasing trend with depth, regardless of bottom water hypoxia (**Figure 2**). The oxygen penetration depth (OPD) ranged from 1 mm (October (Oct) 2015 at DH station) to 29.8 mm (May 2015 at DD2 station) during the normoxia period and from 1.6 mm at DD2 station to 22.8 mm at WM station in Jul 2016 during the hypoxia period (data not shown). No significant spatial or seasonal variations were observed in the OPD. On average, OPDs increased by 76%, ranging from 8.7 mm during bottom water normoxia to 11.6 mm during bottom water hypoxia. Surface

sediments (0–10 mm depth) had higher O_2 concentrations under bottom water normoxia (>150 µmol L^{-1}) than under hypoxia (<50 µmol L^{-1}) (**Figure 2**).

H_2S was detected at both the sediment–water interface and in the sediment, regardless of bottom water hypoxia (**Figure 2**); however, when H_2S was detected during bottom water normoxia, its concentration in the overlying water was lower (<25 µmol L^{-1}) than that during hypoxia (>40 µmol L^{-1}). The maximum sediment H_2S concentration ranged from 180 µmol L^{-1} in Sep 2015 to 840 µmol L^{-1} in August (Aug) 2016 during the hypoxia period and was never greater than 230 µmol L^{-1} in December (Dec) 2018 in the normoxia period (**Figure 2**).

FIGURE 2 | Sediment microelectrode profiles of oxygen (O_2, black circle) and hydrogen sulfide (H_2S, gray square) at DD site in Jinhae Bay from Sep 2015 to Nov 2019 during the sampling period. Results are shown for the **(A)** hypoxia and **(B)** normoxia periods. Note that O_2 and H_2S have different axes (except for profiles generated in Mar 2017). H_2S profiles in Apr 2019 are only available for 1 cm depth into sediments. The top axis is for H_2S, and the bottom axis is for O_2. All profiles derived from DD2 site, except for Sep 2015 (DD1 site).

Sediment Oxygen Consumption

SOC (mean = 16.9 ± 1 mmol O_2 m^{-2} d^{-1}; n = 31, **Table 2**) ranged from 7.4 ± 1.2 mmol O_2 m^{-2} d^{-1} in Jul 2016 to 27.3 ± 2.4 mmol O_2 m^{-2} d^{-1} in Sep 2015 (both data recorded at station DD1). The highest SOC was recorded at site DD in Sep 2015 during bottom water hypoxia. No spatial or seasonal variation was observed in SOC (P > 0.05). SOC was higher in the bottom water hypoxic period than in the bottom water normoxic period (P < 0.05). SOC increased significantly in the hypoxia period by a factor of 27%, from 15.3 ± 1 to 19.5 ± 1.9 mmol O_2 m^{-2} d^{-1}.

Nutrient Fluxes and Nitrification

$NOx(NO_3^- + NO_2^-)$ fluxes varied from -1.15 to 0.42 mmol N m^{-2} d^{-1} with high variability. Overall, sediments were a negligible NOx sink from the overlying water (mean = -0.05 ± 0.05; n = 31, **Table 2**). No spatial or seasonal differences were observed in the net NOx fluxes (P > 0.05). There was no significant exchange of NOx during bottom water normoxia, and the mean NOx flux was negligible, with a value of 0.0003 mmol N m^{-2} d^{-1}; however, under hypoxia, sediments were strong sinks of NOx diffused from the overlying water, with an average rate of -0.14 mmol N m^{-2} d^{-1}. On average, sediments were a netNH_4^+ source in Jinhae Bay (overall mean = 0.46 ± 0.13 mmol N m^{-2} d^{-1}, n = 31, **Table 2**), but variability was high, ranging from -0.79 to 2.49 mmol N m^{-2} d^{-1}. There were no significant differences in the NH_4^+ flux between sites or seasons. Sediments were a consistent source of NH_4^+ in the overlying water at all sites, regardless of season. In general, we measured a decrease of 21% in net ammonium efflux from sediment to overlying water (0.5 mmol N m^{-2} d^{-1} to 0.39 mmol N m^{-2} d^{-1}) during bottom water hypoxia compared with that in normoxia. The estimated nitrification rates averaged 0.18 ± 0.04, ranging from 0 to 0.74 ± 0.28 mmol N m^{-2} d^{-1}. No significant differences in nitrification were observed between the seasons and sampling sites. Overall, under hypoxia, nitrification rates increased by 21% (0.17 mmol N m^{-2} d^{-1} to 0.2 mmol N m^{-2} d^{-1}) compared with that in the normoxic period.

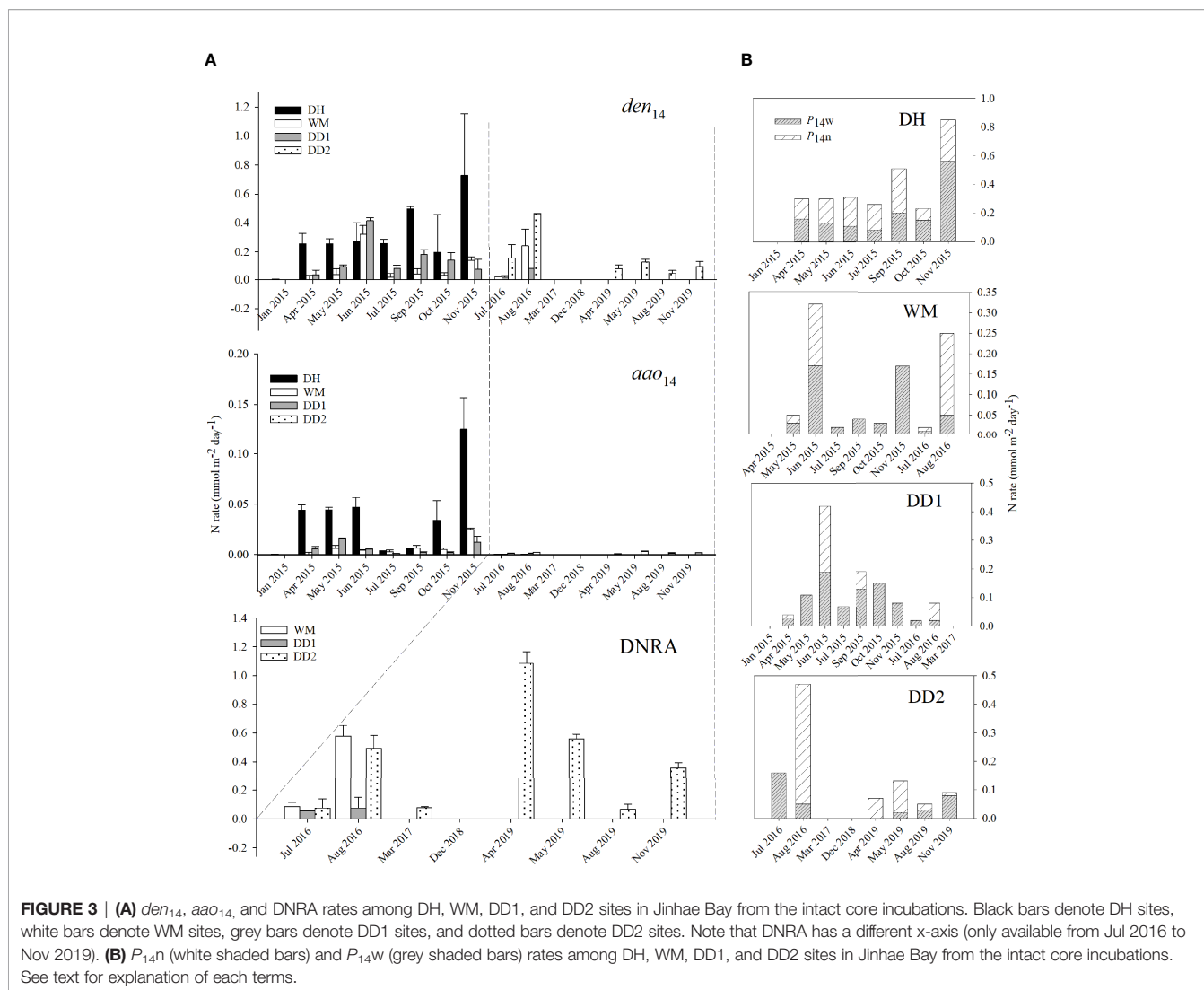## Denitrification, Anammox, and DNRA Rates

Total N_2 production (P_{14}) was mainly sustained by denitrification (**Figure 3**). Denitrification rates ranged from 0 across all four sites to 0.73 mmol N m^{-2} d^{-1} in Nov 2015 at DH with an average value of 0.15 ± 0.03 mmol N m^{-2} d^{-1} (n = 36). There was a pronounced spatial variation in denitrification rates (P = 0.017), with higher rates measured at DH (0.31 ± 0.08 mmol N m^{-2} d^{-1}, n = 8) than at WM (0.09 ± 0.04 mmol N m^{-2} d^{-1}, n = 9), DD1 (0.10 ± 0.04 mmol N m^{-2} d^{-1}, n = 11), or DD2 (0.31 ± 0.08 mmol N m^{-2} d^{-1}, n = 8). There were no significant differences between denitrification rates in different seasons (P > 0.05), although the *den*14 was not detected in winter, while being low in spring (0.09 ± 0.03 mmol N m^{-2} d^{-1}, n = 10), high in summer (0.18 ± 0.04 mmol N m^{-2} d^{-1}, n = 13) and the highest in autumn (0.21 ± 0.07 mmol N m^{-2} d^{-1}, n = 10). Denitrification accounted for 85–100% of total N_2 production (P_{14}) with an average of 93% (n = 30), with 89% recorded at DH, 90% at WM, 94% at DD1, and 99% at DD2 (P < 0.05). There was also a marked seasonal variation in the relative contribution of denitrification to total N_2 production (P_{14}), which was 89% in spring, 91% in autumn, and 97% in summer (P = 0.019). Overall, denitrification rates increased by 75% from the normoxia to hypoxia period (from 0.12 ± 0.03 to 0.21 ± 0.05 mmol N m^{-2} d^{-1}, n = 10, and n = 13, respectively). The relative contribution of denitrification to total N_2 production (P_{14}) also increased during the hypoxia period from 88% to 99% (P = 0.000).

Anammox rates ranged from 0 across all four sites to 0.13 mmol N m^{-2} d^{-1} in Nov 2015 at DH, with an average value of 0.01 ± 0.004 mmol N m^{-2} d^{-1}(n = 36). An obvious spatial variation was observed in anammox rates (P = 0.003), with an average value of 0, 0.01 ± 0.002, and 0.04 ± 0.01 mmol N m^{-2} d^{-1} at DD1 and DD2, WM, and DH, respectively. No seasonal variation was observed between the anammox rates (P > 0.05); however, similar to denitrification, anammox activity was also not detected in winter (n = 3), and was on average very low (nearly 0) in summer (0.005 ± 0.004 mmol N m^{-2} d^{-1}, n = 13) and low in spring (0.01 ± 0.005 mmol N m^{-2} d^{-1}, n = 10) but higher in autumn (0.02 ± 0.01 mmol N m^{-2} d^{-1}, n = 10). On average, anammox only accounted for 7% of total N_2 production (P_{14}), ranging from 2% at DD2 to 11% at DH, 3% in summer, and 11% in spring. Anammox activity decreased significantly from 0.017 ± 0.006 mmol N m^{-2} d^{-1} (n = 23) during the normoxia period to 0.002 ± 0.001 mmol N m^{-2} d^{-1} (n = 13) during the hypoxia period. Anammox only accounted for 1% of the total N_2 production (P_{14}) during the hypoxia period, which was negligible compared to that of the normoxia period (12% of P_{14}). Anammox almost ceased, whereas denitrification increased during the hypoxia period. On the whole, N_2 production (P_{14}) increased by a factor of 55% (0.13 ± 0.04 mmol N m^{-2} d^{-1} (n = 23) to 0.21 ± 0.05 mmol N m^{-2} d^{-1} (n = 13)), which was solely due to the enhancement of denitrification. N_2 production (P_{14}) was mainly sustained by P_{14}w; on average, P_{14}w accounted for 64.13% of total P_{14}. At stations WM and DD1, >75% of the N_2 production (P_{14}) was sustained by P_{14}w, whereas P_{14}n dominated at DH (52%) and DD2 (54%). Both P_{14}w and P_{14}n contributed to the increase in P_{14} during the hypoxia period, of which P_{14}w increased by 28% (from 0.08 ± 0.02 to 0.1 ± 0.02 mmol N m^{-2} d^{-1}), and P_{14}n increased by 93% (from 0.06 ± 0.02 to 0.11 ± 0.04 mmol N m^{-2} d^{-1}).

At station DD2, the DNRA rate peaked at 1.09 ± 0.08 mmol N m^{-2} d^{-1} in April (Apr) 2019, which was 13 times higher than the corresponding denitrification rate. DNRA activity was not detected at DD1 in Mar 2017 and DD2 in Dec 2018, with an overall average value of 0.27 ± 0.09 mmol N m^{-2} d^{-1} from 2015 to 2019 (n = 13, **Figure 3**). No spatial or seasonal variation was observed in DNRA rates (P > 0.05). Overall, DNRA accounted for 61% of the total NO_3^- reduction rate. DNRA contributed 63% at WM and 64% at DD2. Denitrification outperformed DNRA only at DD1 (48%). Compared to those in the normoxia period, DNRA rates decreased by 62% (from 0.38 ± 0.15 to 0.14 ± 0.07 mmol N m^{-2} d^{-1}, **Figure 3**), and the relative contribution of DNRA to total NO_3^- reduction rates decreased from 81% to 58% as well.

FIGURE 3 | **(A)** den_{14}, aao_{14}, and DNRA rates among DH, WM, DD1, and DD2 sites in Jinhae Bay from the intact core incubations. Black bars denote DH sites, white bars denote WM sites, grey bars denote DD1 sites, and dotted bars denote DD2 sites. Note that DNRA has a different x-axis (only available from Jul 2016 to Nov 2019). **(B)** $P_{14}n$ (white shaded bars) and $P_{14}w$ (grey shaded bars) rates among DH, WM, DD1, and DD2 sites in Jinhae Bay from the intact core incubations. See text for explanation of each terms.

Correlations Between Environmental Parameters and Benthic Nitrogen Transformation Rates

Pearson's correlation revealed that bottom water DO content was negatively correlated with bottom water temperature (**Table 3**). Bottom water NH_4^+ concentrations were negatively related to bottom water DO content but positively related to bottom water temperature. den_{14}, $P_{14}n$, P_{14}, and nitrification were positively correlated with bottom water NH_4^+ concentration. A positive correlation was also found among den_{14}, $P_{14}n$, and bottom water temperature. aao_{14} was only positively related to bottom water NOx concentration. A strong negative correlation was observed between the DNRA rate and bottom water salinity. The $P_{14}w$ was positively correlated with bottom water NOx concentration. SOC was negatively correlated with bottom water DO content, whereas it was positively correlated with temperature and NH_4^+ concentration. NOx and NH_4^+ fluxes did not correlate with any of the environmental parameters. Both den_{14} and $aao14$ were positively correlated with $P_{14}w$, $P_{14}n$, P_{14}, and nitrification, whereas aao_{14} was

negatively correlated with SOC. The DNRA rate was positively correlated with SOC and nitrification. Both $P_{14}w$ and $P_{14}n$ were positively correlated with P_{14} and nitrification, while $P_{14}n$ was positively correlated with SOC and negatively correlated with PO_4 flux. The P_{14} and NOx fluxes were positively correlated with nitrification. The SOC was negatively correlated with the NOx flux. A negative correlation was found among the NH_4^+ flux, NOx flux, and nitrification (**Table 3**).

DISCUSSION

Occurrence of "Weak Hypoxia" in Jinhae Bay

A total of 13 episodes of bottom water hypoxia occurred in Jinhae Bay during our survey from 2015 to 2019: ten in the summer and three in the autumn (**Table 1**). Hypoxia in Jinhae Bay is induced by seasonally stratified seawater, mainly due to variations in water column temperature (Kim et al., 2015). Jinhae

TABLE 3 | Pearson's correlation analyses coefficients for ambient bottom water conditions, nutrient fluxes, and nitrogen transformation rates from intact core incubation using Jinhae Bay sediments.

	Temp	Sal	NOx	NH_4	den_{14}	aao_{14}	DNRA	$P_{14}w$	$P_{14}n$	P_{14}	SOC	NOx-f	NH_4-f	Nit	n
DO	-0.729**	-0.20	-0.19	-0.620**	-0.25	0.27	0.13	-0.06	-0.28	-0.20	-0.434**	0.19	0.00	-0.08	37
Temp		-0.14	0.08	0.396**	0.284*	-0.08	0.11	0.13	0.308*	0.25	0.610**	-0.28	0.16	0.02	37
Sal			0.06	0.23	-0.09	-0.10	-0.685**	-0.04	-0.11	-0.09	-0.21	0.24	-0.15	0.13	37
NOx				-0.05	0.20	0.323*	-0.31	0.442**	-0.05	0.22	-0.30	-0.23	0.02	0.11	36
NH_4					0.520**	-0.06	0.11	0.28	0.538**	0.474**	0.341*	-0.06	-0.25	0.372*	36
den_{14}						0.638**	0.44	0.828**	0.896**	0.996**	0.21	-0.18	-0.18	0.725**	36
aao_{14}							.c	0.817**	0.408**	0.702**	-0.375*	0.08	-0.15	0.575**	36
DNRA								-0.04	0.48	0.44	0.738*	0.17	-0.20	0.766*	13
$P_{14}w$									0.501**	0.859**	-0.07	-0.18	-0.01	0.584**	36
$P_{14}n$										0.873**	0.321*	-0.09	-0.30	0.687**	36
P_{14}											0.15	-0.15	-0.18	0.739**	36
SOC												-0.412*	0.29	-0.13	31
NOx-f													-0.433**	0.490**	31
NH_4-f														-0.418**	31
Nit															31

*and **denote $P < 0.05$ and $P < 0.01$ respectively, which were typically regarded as significant, as determined using SPSS version 22.0 program.
c denotes that the value cannot be computed because at least one of the variables is constant.

Bay is a semi-enclosed bay with limited freshwater discharge and relatively high and stable water column salinity ranging from 25–35 psu. Temperature variation played a more significant role than salinity variation in the stratification process. A strong negative correlation between the bottom water oxygen concentration and temperature (**Table 3**, $P < 0.001$), but not salinity, also indicates that bottom water hypoxia is mainly related to temperature variation. Seawater stratification develops in late spring and early summer when the temperature rises, and gradually disappears as the temperature decreases in late fall (Lee et al., 2017).

It is important to note that in shallow Jinhae Bay (mean water depth < 15 m), water column stratification develops but is not very stable (probably in a tidal cycle period range), and as a result, O₂ availability is variable during hypoxia. Although we did not conduct continuous measurement of bottom water oxygen concentration variation during hypoxia periods (from May to Sep), there were seven of 20 normoxia cases (**Table 1**). In particular, we did not capture bottom water hypoxia during the late May 2019 cruise at DD2 station as we expected. More importantly, in six of the 13 episodes of hypoxia, bottom water oxygen concentration was higher than 50 µmol L^{-1}, which is not severe hypoxia (**Table 1**). Taken together, these results indicate that stratification of the water column during hypoxia does not

completely isolate the oxygen supply in the bottom water and sediments, which differs from the situation in other coastal and estuary hypoxia zones (McCarthy et al., 2015; Song et al., 2020) and the permanent oxygen minimum zone (OMZ) in the deep sea (Lam and Kuypers, 2011). Our previous research showed that neither the total abundance of microbes nor the water oxygen demand (WOD) in the water column was affected by hypoxic conditions (Park et al., 2020). Aerobic metabolism was sustained under hypoxia through the intermittent supply of oxygen, and WOD was positively correlated with water temperature, regardless of DO concentration. Unstable hypoxia ("weak hypoxia") in Jinhae Bay, mainly caused by shallow water depth (<15 m) and moderate tidal range (~1.5 m), affects SOC and benthic nitrogen cycling.

Similar to other typical hypoxic areas, hypoxia is accompanied by eutrophication and a peak in bottom water nutrient levels in Jinhae Bay. We summarized and listed the mean concentrations of the water column nutrients (**Table 4**) during hypoxia versus normoxia. The concentrations of NH_4^+ and NOx in the bottom water during hypoxia were 2.9 and 1.3 times than those during normoxia (**Table 4**). NH_4^+ concentration was negatively correlated with the bottom water oxygen concentration and positively correlated with the bottom water temperature (**Table 3**). During hypoxia, organic matter is

TABLE 4 | The mean of ambient nutrient concentrations (µmol L^{-1}) in surface water layer (approximately 0.5 m below the water surface), middle water layer (approximately 6–8 m below the water surface), and bottom water layer (approximately 0.5 m above sediment surface) during hypoxia and normoxia periods in Jinhae Bay.

	NOx			NH_4^+			DIN		
	hypoxia	normoxia	H/N	hypoxia	normoxia	H/N	hypoxia	normoxia	H/N
Sur	1.9 (0.3)	4.5 (0.9)		1.2 (0.2)	2.0 NO0.4)		3.1 (0.3)	6.5 (1)	
Mid	2.6 (0.6)	3.4 (0.6)		2.9 (0.7)	2.0 (0.3)		5.4 (0.9)	5.5 (0.9)	
Bot	4.9 (1.3)	3.7 (0.6)	1.3	7.2 (1.3)	2.5 (0.4)	2.9	12.2(1.5)	6.2 (0.8)	2.0

Sur, surface water layer; Mid, middle water layer; Bot, bottom water layer.
NO_X, nitrate plus nitrite; H/N, hypoxia/normoxia (increase rates of nutrient content change during hypoxia versus normoxia in bottom water layer); N_4^+, ammonium; DIN = NOx plus NH_4^+. Note the values in parentheses represent the standard error of rates measured in duplicate samples.

reduced by sulfate in pore water and produces a variety of soluble substances such as H_2S and NH_3, leading to higher concentrations of inorganic nutrients than those in the original seawater (Presley, 1969; Theede et al., 1969). Kim et al. (2015) suggested that NH_4^+ from the decomposition of surface sediments rich in organic matter diffuses into the overlying water, resulting in the accumulation of NH_4^+ in the bottom water during hypoxia. In addition, the elution rate of nutrients from the sediment was reported to be high at temperatures above 20°C, which triggered a corresponding rapid increase in bottom water nutrient concentrations (Bowie et al., 1985).

Oxygen Penetration Into and Consumption of Sediment

Pore water oxygen declines rapidly with sediment depth and is usually not detectable within a few millimeters of the sediment–water interface (Cai and Sayles, 1996). The O_2 concentration in the bottom water and O_2 consumption process in the sediment determine the degree of O_2 penetration into the sediment. Generally, the OPD was greater when the bottom water oxygen level was high. According to Song et al. (2020), OPDs decrease when the bottom water DO content decreases. Bonaglia et al. (2015) also found a seasonal pattern of deeper oxygen penetration at higher bottom water oxygen concentrations; however, the OPD did not decrease (8.4 mm in the normoxia and 11.6 mm in the hypoxia period) in Jinhae Bay.

The transfer of oxygen from bottom water to the sediment layer can be affected by the presence of macrofauna (Cai and Sayles, 1996). In the current study, bioturbation was allowed by employing intact sediment cores and *in situ* bottom water incubations. Bioturbation can increase the depth of oxygen penetration and affect important biogeochemical processes in the sediments. Li et al. (2016) found thickening of oxidized zones in superficial sediments in the presence of tubificid bioturbation. According to Lim et al. (2007), the total species number and mean density of macrofauna in Jinhae Bay were 255 species and 984 ind. m^{-2}, respectively. The most dominant benthic macrofauna were polychaetes, with a total of 90 species and 773 ind. m^{-2}. Our microelectrode oxygen profiles also provided evidence of biological disturbances, and the fluctuating and discontinuous distribution of pore water oxygen content was due to macrofaunal activity (**Figure 2**).

Some studies have shown that macrofaunal activity is suppressed under hypoxia (Lim et al., 2006; Seo et al., 2015). Although macrofaunal activity may have been inhibited during the hypoxia period, our study indicated that macrofaunal activity did not cease (**Figure 2**). Studies have shown that polychaetes, which are the dominant species in Jinhae Bay, are generally known to be more tolerant to hypoxic stress than other taxonomic groups such as crustaceans (Mangum and Winkle, 1973), amphipods, and echinoderms (Harper et al., 1981). Polychaetes might be able to survive by taking O_2 intermittently. The OPD seemed to be maintained by macrofaunal activity under weak hypoxic conditions.

In the present study, SOC ranged from 7.36 to 27.28 mmol O_2 m^{-2} d^{-1}, which was in the similar but lower range with that of previous studies [43.78–47.40 mmol O_2 m^{-2} d^{-1} reported by Choi et al. (1994) and 32.5–59.1 mmol O_2 m^{-2} d^{-1} reported by Lee et al. (2009)]. This SOC range is consistent with that reported by Lee et al. (2009) for the coastal South Sea of Korea and those of studies from other coastal and estuarine areas (Bonaglia et al., 2014; McCarthy et al., 2015).

Many studies have shown that hypoxic conditions lead to a decrease in the oxygen consumption in sediments. SOC decreases dramatically in both experimentally induced hypoxic conditions (Neubacher et al., 2011; Neubacher et al., 2012; Song et al., 2020) and natural hypoxic events in coastal bays (Foster and Fulweiler, 2019). This decrease is attributed to a reduction in both the concentration gradient across the sediment–water interface and the metabolic activity of aerobic organisms, as well as the contraction of the habitat for aerobic organisms and the suppression of burrowing and irrigating activity of macrofauna under hypoxic conditions (Diaz and Jørgensen, 1992; Diaz and Rosenberg, 2008). A significant negative correlation between SOC and bottom water oxygen content was found in Jinhae Bay (**Table 3**). This is inconsistent with the results of previous studies. The SOC increased by a factor of 27% (P < 0.05) during hypoxia relative to that in normoxia (15.29 to 19.47 mmol O_2 m^{-2} d^{-1}), presumably owing to the "weak hypoxia". As seen in the OPD change, O_2 supply was not limited in the weak hypoxic condition, and organic matter remineralization activity could be enhanced by the rich supply of organic matter (organic matter content was the highest in summer). McCarthy et al. (2013) also reported a negative correlation between SOC and bottom water DO concentration. This negative relationship was explained by the fact that high SOC is driven by abundant fresh organic material and regulates the bottom water oxygen concentration; the fresh organic matter caused the low bottom water DO condition. This view is also supported by our study: the hypoxia period in Jinhae Bay features high levels of organic matter and reduced substances (such as higher concentrations of hydrogen sulfide and ammonium in the bottom water). The positive correlation between SOC and the bottom water ammonium concentration (**Table 3**) is also consistent with the above view. In addition, bottom water temperature and SOC were positively correlated (**Table 3**), indicating that seasonal variability explains this relationship.

Dominant Nitrate Reduction Process in Jinhae Bay

This is the first combined measurement to evaluate denitrification, anammox, DNRA, and nutrient flux rates in Jinhae Bay. Our denitrification rate, 0–0.73 mmol N m^{-2} d^{-1}, is in the range of other reports on the western and southern coasts of Korea (Kim and Yang, 2001; Heo et al., 2011). The overall nitrogen transformation rates were of the same order of magnitude as those reported for the Changjiang estuary, Baltic Sea, and other coastal sediments worldwide (Bonaglia et al., 2014; Song et al., 2020).

DNRA was the dominant pathway for nitrate reduction, accounting for an average of 81% and 58% of total nitrate

reduction during normoxia and hypoxia, respectively. DNRA dominated benthic NO_3^- reduction in Jinhae Bay during both normoxia and hypoxia, which was inconsistent with our initial expectations. In most cases, denitrification dominates the nitrate reduction process in estuarine and coastal marine sediments, as reported in previous studies (McCarthy et al., 2015; Plummer et al., 2015; Song et al., 2020); however, sediments rich in sulfidic and organic matter favor DNRA more than denitrification. For example, DNRA is often dominant in coastal regions with aquaculture systems, such as fish, mussels, and shrimp farms, which may supply a high loading of labile organic matter in sediments (Christensen et al., 2000; Nizzoli et al., 2006; Gao et al., 2019).

It is well known that Jinhae Bay is the most important aquaculture site in Korea, and shellfish farming provides a rich source of organic matter. Accordingly, sediment characteristic experiments suggested that the sediments were fine-grained and rich in organic matter (from 12% to 18% dry weight). The H_2S profiles (**Figure 2**) demonstrated the widespread distribution of sulfides in the sediments of Jinhae Bay, regardless of bottom water hypoxia. Sulfides can inhibit nitrification, namely, coupled nitrification–denitrification, but stimulate DNRA; hence, DNRA is favored over denitrification in the presence of sulfate-reducing bacteria (Brunet and Garcia-Gil, 1996). Consequently, DNRA is always the dominant nitrate reduction pathway in Jinhae Bay; however, DNRA dominance decreased during hypoxia owing to enhanced denitrification (described below).

Enhanced Denitrification During Hypoxia

In Jinhae Bay, denitrification rates increased significantly by a factor of 75% under hypoxia, from 0.12 to 0.21 mmol N m^{-2} d^{-1} (**Figure 4**). The enhanced denitrification rates can be explained by the nitrification activity, as suggested by the strong positive correlation between denitrification and ammonium concentration (**Table 3**, P < 0.001). In general, this was expected because denitrification in marine sediments is coupled with nitrification and coupled nitrification–denitrification is often the dominant denitrification pathway. High NH_4^+ availability enhances nitrification activity when O_2 is less limiting, thereby stimulating a high denitrification rate. During hypoxia, $P_{14}n$ increased by 93% (from 0.06 to 0.11 mmol N m^{-2} d^{-1}), while $P_{14}w$ only increased by 28% (from 0.06 to 0.11 mmol N m^{-2} d^{-1}), although the bottom water NOx concentration increased significantly. Therefore, the enhanced denitrification rate was mainly due to the increase in coupled nitrification–denitrification.

Nitrification is an aerobic process that occurs in the oxic layer, usually in the upper few millimeters of the sediment, and regulates the denitrification pathway in estuarine and coastal sediments by providing the substrate (NO_3^-) required for denitrification (Hansen et al., 1981). Typically, the availability of oxygen in the bottom water regulates nitrification activity, and hypoxia inhibits the nitrification rate; therefore, the nitrification-coupled denitrification rate also decreases. Song et al. (2020) reported an obvious repression in both sedimentary nitrification and benthic nitrogen loss under severely hypoxic conditions compared to those of oxic and/or ambient conditions. Interestingly, the efflux of ammonium decreased by 21% during hypoxia, which would suggest that nitrification in the sediment was not suppressed under the weak hypoxic conditions. Correspondingly, nitrification increased by 21% (from 0.17 to 0.2 mmol N m^{-2} d^{-1}) during the hypoxia period in Jinhae Bay (**Figure 4**).

Nitrification has been reported to occur at extremely low oxygen concentrations and is often the fastest under
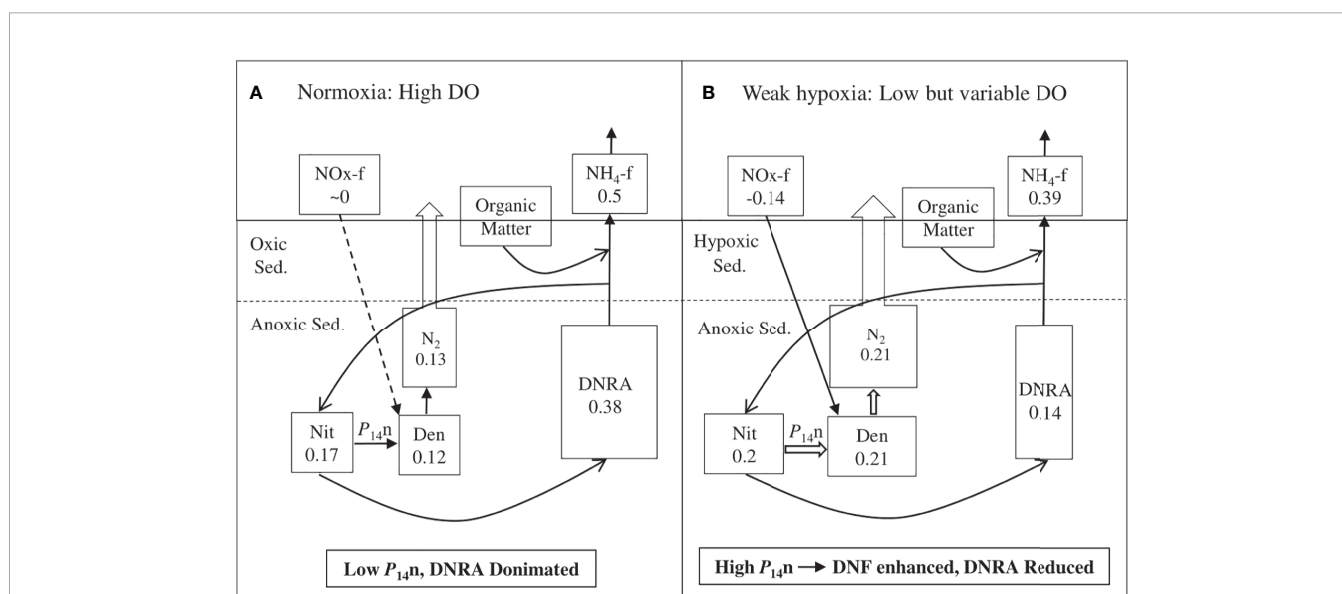
FIGURE 4 | Representation of principal annual nitrogen pathways and their rates investigated from 2015 to 2019 in Jinhae Bay during **(A)** normoxia and **(B)** weak hypoxia periods. Unit: mmol N m^{-2} d^{-1} for related benthic nitrogen transformations. DNF denotes denitrification, DNRA denotes dissimilatory nitrate reduction to ammonium.

subsaturating oxygen conditions (Goreau et al., 1980; Kester et al., 1997; Bristow et al., 2016). Higher rates of potential nitrification in the hypoxic or anoxic treatment than in the oxic treatment were confirmed by Caffrey et al. (2019) in a chronically hypoxic basin in Roskilde Fjord, Denmark. This implies that nitrifiers may be able to recover rapidly from low oxygen stress. Some studies have shown that bacteria exposed to hypoxia or anoxia have a higher affinity for oxygen than bacteria from permanently oxic environments, which may be due to physiological adaptations of nitrification communities to anoxic environments (Bodelier et al., 1996). Our results showing that nitrification increased during hypoxia were consistent with those of the studies above. Therefore, weak hypoxia in Jinhae Bay favors enhanced nitrification activity.

In Jinhae Bay, enhanced nitrification rates during the hypoxia period can also be explained by depressed macrofaunal activity. Macrofaunal activity contributes to the transport of NH_4^+ from burrows into the water column, thus reducing the availability of NH_4^+ (the substrate that can be used for nitrification) in sediment, which results in a short circuit in the coupled nitrification–denitrification process (Mermillod-Blondin et al., 2004; Owens and Cornwell, 2020). The effects of bioturbation were demonstrated in Chesapeake Bay, where Owens and Cornwell found that high bioirrigation rates reduced the denitrification efficiency. At very high rates of bioirrigation in June, most DIN escaped into the water column as NH_4^+. The denitrification efficiency reduced to 30%, but the high denitrification efficiency was maintained at a moderate bioirrigation rate in spring, and most of the DIN returned to the water column in the form of N_2 (Owens and Cornwell, 2020). This bioirrigation effect was also observed in the present study. Nitrification increased by a factor of 21% with depressed NH_4^+ efflux, and more DIN was removed in the form of N_2 when macrofaunal activity was depressed during hypoxia. In addition, the overall nitrification rates were positively correlated with bottom water NH_4^+ concentration (**Table 3**), suggesting that the availability of NH_4^+ could affect nitrification activity, and high NH_4^+ availability during hypoxia can directly stimulate nitrification. However, the spatial heterogeneity of the bioturbation is common and might obscure the seasonal trends.

Denitrification in marine sediments is a temperature-dependent process (Rysgaard et al., 2004). The positive correlation between denitrification and temperature indicates that high ambient temperatures can accelerate the activity of denitrifying bacteria (**Table 3**). The effect of temperature variation on denitrification activity was also demonstrated by Neubacher et al. (2013) and Bonaglia et al. (2014). Denitrification activity under hypoxic conditions has been reported to be diminished (Jäntti and Hietanen, 2012; Bonaglia et al., 2014; Song et al., 2020), enhanced (McCarthy et al., 2008; Neubacher et al., 2011; Neubacher et al., 2012; McCarthy et al., 2015), or almost unchanged (Foster and Fulweiler, 2019). These inconsistencies in response to hypoxia are possibly due to site-specific environmental conditions, such as nitrate availability, temperature, sediment organic matter, and the degree of hypoxia and duration of hypoxia exposure. In Jinhae Bay, increased denitrification is mainly due to enhanced NH_4^+ availability, which favors nitrification during weak hypoxia.

Ammonium Budget and Related Process During Hypoxia

The sediment was a source of DIN in the form of NH_4^+ in the overlying water (0.5 and 0.25 mmol N m^{-2} d^{-1} during normoxia and hypoxia, respectively), regardless of bottom water hypoxia; however, the fact that the sediments were consistent sources of ammonium throughout the year under ambient oxygen in Jinhae Bay, even outside the hypoxia period, may indicate a long-term negative effect on the nitrifying community in the sediment (Caffrey et al., 2003; Greenwood et al., 2010). NH_4^+ efflux decreased by 21%, and a complete cessation of the efflux of nitrate from sediments was during the hypoxia period. The depressed NH_4^+ effluxes during the hypoxia period in Jinhae Bay are typically attributed to increased NH_4^+ uptake through nitrification and decreased NH_4^+ production from DNRA. As described in the previous section, nitrification rates increased by 21%, which contributed to the reduced NH_4^+ efflux during hypoxia.

Correspondingly, DNRA decreased by 62% during the hypoxia period. The decreased DNRA activity was consistent with depressed NH_4^+ effluxes during hypoxia. Under hypoxic conditions, sulfide can quickly combine with Fe (II) to produce FeS precipitates. This non-biological reaction can occur quickly, reducing the bioavailability of free sulfide for DNRA activity (Brunet and Garcia-Gil, 1996). Another possible explanation might be the depressed macrofaunal activity during hypoxia. The cycling of fresh organic matter in sediments has beenhown to be greatly enhanced by the activity of macrofauna (Heilskov, 2001). Studies have shown that the stimulating effect of "high-quality" fresh organic matter on DNRA may be more important than the content of organic matter (Gao et al., 2019). The inhibited macrofaunal activity during hypoxia might reduce the cycling of fresh organic matter in sediments, even though the organic matter content was slightly higher than that in normoxia. Therefore, the DNRA rate decreased during hypoxia but was still higher than the denitrification rate and was the dominant pathway in the nitrate reduction process.

Reactive Nitrogen Loss During Hypoxia

Under hypoxia, there was a 55% increase in the total N_2 gas production (loss of reactive nitrogen). The measured increase in total N_2 production (P_{14}) during hypoxia was solely due to an increase in denitrification activity, as anammox activity decreased from 0.01 mmol N m^{-2} d^{-1} to below detection (denitrification increased by 75%, while anammox ceased). Anammox, when occurring, does not exceed 15% of total nitrogen production and is negligible compared to denitrification. Denitrification dominates the total nitrogen production in Jinhae Bay, which is consistent with benthic nitrogen cycling in other estuarine and coastal sediments (Neubacher et al., 2011; Neubacher et al., 2012; Bonaglia et al., 2014; Song et al., 2020). Enhanced denitrification and diminished anammox during hypoxia may be explained by the fact that most

known denitrifying bacteria are facultative anaerobic organisms that can respire using both oxygen and nitrate (Körner and Zumft, 1989). Hypoxic stress can induce aerobic heterotrophic denitrifying bacteria to respond to any available nitrate, thus readily exploiting the newly expanded anoxic zone (Haürtig and Zumft, 1999); however, it appears that anammox bacteria, known as obligate anaerobes, were unable to exploit the newly extended suboxic sediment layer. In addition, anammox activity is constrained by the availability of nitrite; hence, active anammox bacteria are likely to concentrate in the narrow zone where nitrate reduction activity is high and nitrite availability is maximal immediately below the oxic surface layer (Meyer et al., 2005). The positive correlation between the overall anammox rates and bottom water NOx concentration also indicated the dependence of anammox activity on nitrite availability (**Table 3**).

CONCLUSIONS

Seasonal bottom water hypoxia has been reported to occur annually in Jinhae Bay owing to water column stratification (mainly caused by temperature variation); however, because of the shallow water depth in Jinhae Bay, the oxygen in the bottom water and sediments is not completely blocked, even in summer when hypoxia occurs. This condition is significantly different from other deep coastal hypoxic zones and the OMZ; therefore, we defined it as "weak hypoxia". The O_2 microelectrode profiles indicated the existence of biodisturbance. Macrofauna may maintain a deep OPD and high SOC through occasional intermittent oxygen supply under weak hypoxic conditions, together with other factors such as high organic matter content and temperature.

The increase in denitrification rate during the hypoxia period was mainly due to the significant increase in coupled nitrification–denitrification (P_{14}n increased by 93%, whereas P_{14}w only increased by 28%). The enhancement of nitrification showed that weak hypoxia did not inhibit nitrification activity, and nitrifying bacteria could use the intermittent oxygen supply. The dominance of DNRA in the nitrate reduction process was mainly due to the sulfidic and rich organic matter sediments in Jinhae Bay. The overall dominance of DNRA might have promoted the formation and maintenance of hypoxia.

Enhanced denitrification during hypoxia contributes to an increase in the removal of reactive nitrogen and reduces the release of recycled inorganic nitrogen to the water column, which may help alleviate hypoxia and eutrophication, as well as regulate primary production in the area.

Taken together, these results indicate that hypoxia can increase nitrogen loss in the form of N_2 gas and suppress inorganic nitrogen recycling. When the O_2 supply is not completely blocked, it contributes to nitrogen loss and alleviates eutrophication in the area.

DATA AVAILABILITY STATEMENT

The original contributions presented in the study are included in the article/supplementary material. Further inquiries can be directed to the corresponding author.

AUTHOR CONTRIBUTIONS

SA contributed to experimental design, sampling, and revision of the manuscript. YH performed sampling, experiments, and data analysis and wrote the manuscript. All authors contributed to the article and approved the submitted version.

FUNDING

ACKNOWLEDGMENTS

REFERENCES

An, S., and Gardner, W. S. (2002). Dissimilatory Nitrate Reduction to Ammonium (DNRA) as a Nitrogen Link, Versus Denitrification as a Sink in a Shallow Estuary (Laguna Madre/Baffin Bay, Texas). *Mar. Ecol. Prog. Ser.* 237, 41–50. doi: 10.3354/meps237041

An, S., and Joye, S. B. (2001). Enhancement of Coupled Nitrification-Denitrification by Benthic Photosynthesis in Shallow Estuarine Sediments. *Limnol. Oceanogr.* 46, 62–74. doi: 10.4319/lo.2001.46.1.0062

Bae, W., Baek, S., Chung, J., and Lee, Y. (2001). Optimal Operational Factors for Nitrite Accumulation in Batch Reactors. *Biodegradation* 12, 359–366. doi: 10.1023/A:1014308229656

Bodelier, P., Libochant, J. A., Blom, C., and Laanbroek, H. J. (1996). Dynamics of Nitrification and Denitrification in Root-Oxygenated Sediments and Adaptation of Ammonia-Oxidizing Bacteria to Low-Oxygen or Anoxic

Habitats. *Appl. Environ. Microbiol.* 62, 4100–4107. doi: 10.1128/aem.62.11.4100-4107.1996

Bonaglia, S., Deutsch, B., Bartoli, M., Marchant, H. K., and Brüchert, V. (2014). Seasonal Oxygen, Nitrogen and Phosphorus Benthic Cycling Along an Impacted Baltic Sea Estuary: Regulation and Spatial Patterns. *Biogeochemistry* 119, 139–160. doi: 10.1007/s10533-014-9953-6

Bowie, G. L., Mills, W. B., Porcella, D. B., Campbell, C. L., Pagenkopf, J. R., Rupp, G. L., et al. (1985). *Rates, Constants, and Kinetics Formulations in Surface Water Quality Modeling* (Washington, DC: EPA).

Breitburg, D., Levin, L. A., Oschlies, A., Gregoire, M., Chavez, F. P., Conley, D. J., et al. (2018). Declining Oxygen in the Global Ocean and Coastal Waters. *Science* 359, eeam7240. doi: 10.1126/science.aam7240

Bristow, L. A., Dalsgaard, T., Tiano, L., Mills, D. B., Bertagnolli, A. D., Wright, J. J., et al. (2016). Ammonium and Nitrite Oxidation at Nanomolar Oxygen

Concentrations in Oxygen Minimum Zone Waters. *Proc. Natl. Acad. Sci. U. S. A.* 113, 10601–10606. doi: 10.1073/pnas.1600359113

Brunet, R., and Garcia-Gil, L. (1996). Sulfide-Induced Dissimilatory Nitrate Reduction to Ammonia in Anaerobic Freshwater Sediments. *FEMS Microbiol. Ecol.* 21, 131–138. doi: 10.1128/AEM.00782-17

Caffrey, J. M., Bonaglia, S., and Conley, D. J. (2019). Short Exposure to Oxygen and Sulfide Alter Nitrification, Denitrification, and DNRA Activity in Seasonally Hypoxic Estuarine Sediments. *FEMS Microbiol. Lett.* 366, 1–10. doi: 10.1093/femsle/fny288

Caffrey, J. M., Harrington, N., Solem, I., and Ward, B. B. (2003). Biogeochemical Processes in a Small California Estuary. 2. Nitrification Activity, Community Structure and Role in Nitrogen Budgets. *Mar. Ecol. Prog. Ser.* 248, 27–40. doi: 10.3354/meps248027

Cai, W.-J., and Sayles, F. L. (1996). Oxygen Penetration Depths and Fluxes in Marine Sediments. *Mar. Chem.* 52, 123–131. doi: 10.1016/0304-4203(95)00081-X

Cho, H. Y., Chae, J. W., and Chun, S. Y. (2002). Stratification and DO Concentration Change in Chinhae-Masan Bay. *J. Kor. Soc Coast. Ocean. Eng.* 14, 295–307.

Choi, W. J., Park, C. K., and Lee, S. M. (1994). Numerical Simulation of the Formation of Oxygen Deficient Water-Masses in Jinhae Bay. *Bull. Kor. Fish. Soc* 27, 413–433.

Christensen, P. B., Rysgaard, S., Sloth, N. P., Dalsgaard, T., and Schwærter, S. (2000). Sediment Mineralization, Nutrient Fluxes, Denitrification and Dissimilatory Nitrate Reduction to Ammonium in an Estuarine Fjord With Sea Cage Trout Farms. *Aquat. Microb. Ecol.* 21, 73–84. doi: 10.3354/ame021073

Deng, F., Hou, L., Liu, M., Zheng, Y., Yin, G., Li, X., et al. (2015). Dissimilatory Nitrate Reduction Processes and Associated Contribution to Nitrogen Removal in Sediments of the Yangtze Estuary. *J. Geophys. Res. Biogeosci.* 120, 1521–1531. doi: 10.1002/2015jg003007

Diaz, R. J., and Rosenberg, R. (1995). Marine Benthic Hypoxia: A Review of its Ecological Effects and the Behavioural Responses of Benthic Macrofauna. *Oceanogr. Mar. Biol. Annu. Rev.* 33, 245–203.

Diaz, R. J., and Rosenberg, R. (2008). Spreading Dead Zones and Consequences for Marine Ecosystems. *Science* 321, 926–929. doi: 10.1126/science.1156401

Eugster, O., and Gruber, N. (2012). A Probabilistic Estimate of Global Marine N-Fixation and Denitrification. *Global Biogeochem. Cycle.* 26, GB4013. doi: 10.1029/2012gb004300

Foster, S. Q., and Fulweiler, R. W. (2019). Estuarine Sediments Exhibit Dynamic and Variable Biogeochemical Responses to Hypoxia. *J. Geophys. Res. Biogeosci.* 124, 737–758. doi: 10.1029/2018jg004663

Galton, D. (1884). 10th Meeting:-"Report of the Royal Commission on Metropolitan Sewage". *J. Soc Art.* 33, 290–299.

Gao, D., Liu, M., Hou, L., Derrick, Y. F. L., Wang, W., Li, X., et al. (2019). Effects of Shrimp-Aquaculture Reclamation on Sediment Nitrate Dissimilatory Reduction Processes in a Coastal Wetland of Southeastern China. *Environ. Pollut.* 255, 113219. doi: 10.1016/j.envpol.2019.113219

Goreau, T. J., Kaplan, W. A., Wofsy, S. C., McElroy, M. B., Valois, F. W., and Watson, S. W. (1980). Production of NO_2-And N_2O by Nitrifying Bacteria at Reduced Concentrations of Oxygen. *Appl. Environ. Microbiol.* 40, 526–532. doi: 10.1128/aem.40.3.526-532.1980

Greenwood, N., Parker, E. R., Fernand, L., Sivyer, D. B., Weston, K., Painting, S. J., et al. (2010). Detection of Low Bottom Water Oxygen Concentrations in the North Sea; Implications for Monitoring and Assessment of Ecosystem Health. *Biogeosciences* 7, 1357–1373. doi: 10.5194/bg-7-1357-2010

Haürtig, E., and Zumft, W. G. (1999). Kinetics of nirS Expression (Cytochrome Cd 1 Nitrite Reductase) in Pseudomonas Stutzeri During the Transition From Aerobic Respiration to Denitrification: Evidence for a Denitrification-Specific Nitrate-And Nitrite-Responsive Regulatory System. *J. Bacteriol.* 181, 161–166. doi: 10.1128/JB.181.1.161-166.1999

Hansen, J. I., Henriksen, K., and Blackburn, T. H. (1981). Seasonal Distribution of Nitrifying Bacteria and Rates of Nitrification in Coastal Marine Sediments. *Microb. Ecol.* 7, 297–304. doi: 10.1007/bf02341424

Harper, D. E.Jr., McKinney, L. D., Salzer, R. R., and Case, R. (1981). The Occurrence of Hypoxic Bottom Water Off the Upper Texas Coast and Its Effects on the Benthic Biota. *Contrib. Mar. Sci.* 24, 53–79. doi: http://hdl.handle.net/1969.3/20847

Hasler, A. D. (1969). Cultural Eutrophication Is Reversible. *Bioscience* 19, 425–431. doi: 10.2307/1294478

Heilskov, A. (2001). Effects of Benthic Fauna on Organic Matter Mineralization in Fish-Farm Sediments: Importance of Size and Abundance. *ICES. J. Mar. Sci.* 58, 427–434. doi: 10.1006/jmsc.2000.1026

Helm, K. P., Bindoff, N. L., and Church, J. A. (2011). Observed Decreases in Oxygen Content of the Global Ocean. *Geophys. Res. Lett.* 38, L23602. doi: 10.1029/2011gl049513

Heo, N., Lee, J., Choi, J., and An, S. (2011). Nitrogen Removal *via* Sediment Denitrification and Its Seasonal Variations in Major Estuaries of South Coast of Korean Peninsula. *Sea.* 16, 81–96. doi: 10.7850/jkso.12011.16.2.081

Hietanen, S., and Lukkari, K. (2007). Effects of Short-Term Anoxia on Benthic Denitrification, Nutrient Fluxes and Phosphorus Forms in Coastal Baltic Sediment. *Aquat. Microb. Ecol.* 49, 293–302. doi: 10.3354/ame01146

Jäntti, H., and Hietanen, S. (2012). The Effects of Hypoxia on Sediment Nitrogen Cycling in the Baltic Sea. *Ambio* 41, 161–169. doi: 10.1007/s13280-011-0233-6

Jensen, M. M., Kuypers, M. M., Gaute, L., and Thamdrup, B. (2008). Rates and Regulation of Anaerobic Ammonium Oxidation and Denitrification in the Black Sea. *Limnol. Oceanogr.* 53, 23–36. doi: 10.4319/lo.2008.53.1.0023

Kana, T. M., Darkangelo, C., Hunt, M. D., Oldham, J. B., Bennett, G. E., and Cornwell, J. C. (1994). Membrane Inlet Mass Spectrometer for Rapid High-Precision Determination of N_2, O_2, and Ar in Environmental Water Samples. *Anal. Chem.* 66, 4166–4170. doi: 10.1021/ac00095a009

Kemp, W. M., Boynton, W. R., Adolf, J. E., Boesch, D. F., Boicourt, W. C., Brush, G., et al. (2005). Eutrophication of Chesapeake Bay: Historical Trends and Ecological Interactions. *Mar. Ecol. Prog. Ser.* 303, 1–29. doi: 10.3354/meps303001

Kemp, W., Testa, J. M., Conley, D. J., Gilbert, D., and Hagy, J. D. (2009). Temporal Responses of Coastal Hypoxia to Nutrient Loading and Physical Controls. *Biogeosciences* 6, 2985–3008. doi: 10.5194/bg-6-2985-2009

Kester, R. A., De Boer, W., and Laanbroek, H. J. (1997). Production of NO and N (Inf2) O by Pure Cultures of Nitrifying and Denitrifying Bacteria During Changes in Aeration. *Appl. Environ. Microbiol.* 63, 3872–3877. doi: 10.1089/oli.1.1997.7.523

Kim, D., Choi, H. W., Choi, S. H., Baek, S. H., Kim, K. H., Jeong, J. H., et al. (2013). Spatial and Seasonal Variations in the Water Quality of Jinhae Bay, Korea. *N. Z. J. Mar. Freshwat. Res.* 47, 192–207. doi: 10.1080/00288330.2013.772066

Kim, Y. S., Lee, Y. H., Kwon, J. N., and Choi, H. G. (2015). The Effect of Low Oxygen Conditions on Biogeochemical Cycling of Nutrients in a Shallow Seasonally Stratified Bay in Southeast Korea (Jinhae Bay). *Mar. Pollut. Bull.* 95, 333–341. doi: 10.1016/j.marpolbul.2015.03.022

Kim, D., and Yang, J. (2001). Denitrification and COD, TN and SS Fluxes in Komso Bay, Korea. *Kor. Soc Mar. Environ. Energy* 4, 32–41.

Körner, H., and Zumft, W. G. (1989). Expression of Denitrification Enzymes in Response to the Dissolved Oxygen Level and Respiratory Substrate in Continuous Culture of Pseudomonas Stutzeri. *Appl. Environ. Microbiol.* 55, 1670–1676. doi: 10.1128/aem.55.7.1670-1676.1989

Kwon, H. K., Kim, G., Lim, W. A., Park, J. W., and Park, T. G. (2020). Conditions of Nutrients and Dissolved Organic Matter for the Outbreaks of Paralytic Shellfish Poisoning (PSP) in Jinhae Bay, Korea. *Mar. Pollut. Bull.* 158, 111381. doi: 10.1016/j.marpolbul.2020.111381

Lam, P., and Kuypers, M. M. (2011). Microbial Nitrogen Cycling Processes in Oxygen Minimum Zones. *Ann. Rev. Mar. Sci.* 3, 317–345. doi: 10.1146/annurev-marine-120709-142814

Lee, J., Kim, S.-G., and An, S. (2017). Dynamics of the Physical and Biogeochemical Processes During Hypoxia in Jinhae Bay, South Korea. *J. Coast. Res.* 33, 854–863. doi: 10.2112/jcoastres-d-16-00122.1

Lee, J., Kim, S., Kim, S.-S., An, S., Kim, Y.-T., and Choi, O.-I. (2009). Sediment Oxygen Consumption in Semi-Closed Korean Coastal Bays During Summer. *Ocean. Sci. J.* 44, 161–171. doi: 10.1007/s12601-009-0014-3

Lee, J., Park, K.-T., Lim, J.-H., and Kim, I.-N. (2018). Hypoxia in Korean Coastal Waters: A Case Study of the Natural Jinhae Bay and Artificial Shihwa Bay. *Front. Mar. Sci.* 5. doi: 10.3389/fmars.2018.00070

Li, Y., Hua, X., Zheng, F., Dong, D., Liang, D., and Guo, Z. (2016). Effects of Tubificid Bioturbation on Pore Structures in Sediment and the Migration of Sediment Particles. *Environ. Sci. Pollut. Res. Int.* 23, 8064–8075. doi: 10.1007/s11356-015-5949-6

Lim, H. S., Diaz, R. J., Hong, J. S., and Schaffner, L. C. (2006). Hypoxia and Benthic Community Recovery in Korean Coastal Waters. *Mar. Pollut. Bull.* 52, 1517–1526. doi: 10.1016/j.marpolbul.2006.05.013

Lim, K.-H., Shin, H.-C., Yoon, S.-M., and Koh, C.-H. (2007). Assessment of Benthic Environment Based on Macrobenthic Community Analysis in Jinhae Bay, Korea. *Sea.* 12, 9–23.

Mangum, C., and Winkle, W. V. (1973). Responses of Aquatic Invertebrates to Declining Oxygen Conditions. *Am. Zool.* 13, 529–541. doi: 10.1093/icb/13.2.529

McCarthy, M. J., Carini, S. A., Liu, Z., Ostrom, N. E., and Gardner, W. S. (2013). Oxygen Consumption in the Water Column and Sediments of the Northern Gulf of Mexico Hypoxic Zone. *Estuar. Coast. Shelf. Sci.* 123, 46–53. doi: 10.1016/j.ecss.2013.02.019

McCarthy, M. J., McNeal, K. S., Morse, J. W., and Gardner, W. S. (2008). Bottom-Water Hypoxia Effects on Sediment–Water Interface Nitrogen Transformations in a Seasonally Hypoxic, Shallow Bay (Corpus Christi Bay, TX, USA). *Estuar. Coast.* 31, 521–531. doi: 10.1007/s12237-008-9041-z

McCarthy, M. J., Newell, S. E., Carini, S. A., and Gardner, W. S. (2015). Denitrification Dominates Sediment Nitrogen Removal and Is Enhanced by Bottom-Water Hypoxia in the Northern Gulf of Mexico. *Estuar. Coast.* 38, 2279–2294. doi: 10.1007/s12237-015-9964-0

Mermillod-Blondin, F., Rosenberg, R., François-Carcaillet, F., Norling, K., and Mauclaire, L. (2004). Influence of Bioturbation by Three Benthic Infaunal Species on Microbial Communities and Biogeochemical Processes in Marine Sediment. *Aquat. Microb. Ecol.* 36, 271–284. doi: 10.3354/ame036271

Meyer, R. L., Risgaard-Petersen, N., and Allen, D. E. (2005). Correlation Between Anammox Activity and Microscale Distribution of Nitrite in a Subtropical Mangrove Sediment. *Appl. Environ. Microbiol.* 71, 6142–6149. doi: 10.1128/AEM.71.10.6142-6149.2005

Neubacher, E. C., Parker, R. E., and Trimmer, M. (2011). Short-Term Hypoxia Alters the Balance of the Nitrogen Cycle in Coastal Sediments. *Limnol. Oceanogr.* 56, 651–665. doi: 10.4319/lo.2011.56.2.0651

Neubacher, E. C., Parker, R. E., and Trimmer, M. (2012). The Potential Effect of Sustained Hypoxia on Nitrogen Cycling in Sediment From the Southern North Sea: A Mesocosm Experiment. *Biogeochemistry* 113, 69–84. doi: 10.1007/s10533-012-9749-5

Nizzoli, D., Welsh, D. T., Fano, E. A., and Viaroli, P. (2006). Impact of Clam and Mussel Farming on Benthic Metabolism and Nitrogen Cycling, With Emphasis on Nitrate Reduction Pathways. *Mar. Ecol. Prog. Ser.* 315, 151–165. doi: 10.3354/meps315151

Owens, M. S., and Cornwell, J. C. (2020). Temporal Enhancement of Denitrification in Bioirrigated Estuarine Sediments. *Aquat. Sci.* 82, 1–12. doi: 10.1007/s00027-020-00742-y

Park, Y., Cha, J., Song, B., Huang, Y., Kim, S., Kim, S., et al. (2020). Total Microbial Activity and Sulfur Cycling Microbe Changes in Response to the Development of Hypoxia in a Shallow Estuary. *Ocean. Sci. J.* 55, 165–181. doi: 10.1007/s12601-020-0011-0

Parsons, T. R., Maita, Y., and Carol, C. M. (1984). *A Manual of Chemical and Biological Method for Seawater Analysis* (Oxford: Pergamon Press).

Plummer, P., Tobias, C., and Cady, D. (2015). Nitrogen Reduction Pathways in Estuarine Sediments: Influences of Organic Carbon and Sulfide. *J. Geophys. Res. Biogeosci.* 120, 1958–1972. doi: 10.1002/2015jg003057

Presley, B. J. (1969). *Chemistry of Interstitial Water From Marine Sediments.[dissertation]* (Los Angeles (CA): University of California Los Angeles).

Rabalais, N., Diaz, R. J., Levin, L., Turner, R. E., Gilbert, D., and Zhang, J. (2010). Dynamics and Distribution of Natural and Human-Caused Hypoxia. *Biogeosciences* 7, 585–619. doi: 10.5194/bg-7-585-2010

Rabalais, N., Turner, R., Sen Gupta, B., Boesch, D., Chapman, P., and Murrell, M. (2007). Characterization and Long-Term Trends of Hypoxia in the Northern Gulf of Mexico: Does the Science Support the Action Plan? *Estuar. Coast.* 30, 753–772. doi: 10.1007/BF02841332

Risgaard-Petersen, N., Nielsen, L. P., Rysgaard, S., Dalsgaard, T., and Meyer, R. L. (2003). Application of the Isotope Pairing Technique in Sediments Where Anammox and Denitrification Coexist. *Limnol. Oceanogr. Methods* 1, 63–73. doi: 10.4319/lom.2003.1.63Citations:128

Rysgaard, S., Glud, R. N., Risgaard-Petersen, N., and Dalsgaard, T. (2004). Denitrification and Anammox Activity in Arctic Marine Sediments. *Limnol. Oceanogr.* 49, 1493–1502. doi: 10.4319/lo.2004.49.5.1493

Schmidtko, S., Stramma, L., and Visbeck, M. (2017). Decline in Global Oceanic Oxygen Content During the Past Five Decades. *Nature* 542, 335–339. doi: 10.1038/nature21399

Seo, J.-Y., Lim, H.-S., and Choi, J.-W. (2015). Spatio-Temporal Distribution of Macrobenthic Communities in Jinhae Bay, Korea. *Ocean. Polar. Res.* 37, 295–315. doi: 10.4217/opr.2015.37.4.295

Shan, J., Zhao, X., Sheng, R., Xia, Y., Ti, C., Quan, X., et al. (2016). Dissimilatory Nitrate Reduction Processes in Typical Chinese Paddy Soils: Rates, Relative Contributions, and Influencing Factors. *Environ. Sci. Technol.* 50, 9972–9980. doi: 10.1021/acs.est.6b01765

Song, G., Liu, S., Zhang, J., Zhu, Z., Zhang, G., Marchant, H. K., et al. (2020). Response of Benthic Nitrogen Cycling to Estuarine Hypoxia. *Limnol. Oceanogr.* 66, 652–666. doi: 10.1002/lno.11630

Strickland, J. D. H., and Parsons, T. R. (1972). *A Practical Handbook of Seawater Analysis* (Ottawa: Fisheries Research Board of Canada).

Thamdrup, B., and Dalsgaard, T. (2002). Production of N(2) Through Anaerobic Ammonium Oxidation Coupled to Nitrate Reduction in Marine Sediments. *Appl. Environ. Microbiol.* 68, 1312–1318. doi: 10.1128/AEM.68.3.1312-1318.2002

Theede, H., Ponat, A., Hiroki, K., and Schlieper, C. (1969). Studies on the Resistance of Marine Bottom Invertebrates to Oxygen-Deficiency and Hydrogen Sulphide. *Mar. Biol.* 2, 325–337. doi: 10.1007/BF00355712

Tong, L., and Zhang, J. (2007). Chinese IMBER/GLOBEC Program Progress Dead Zone Survey. *IMBER. Update* 6, 6–8.

Wang, S., Pi, Y., Song, Y., Jiang, Y., Zhou, L., Liu, W., et al. (2020). Hotspot of Dissimilatory Nitrate Reduction to Ammonium (DNRA) Process in Freshwater Sediments of Riparian Zones. *Water Res.* 173, 115539. doi: 10.1016/j.watres.2020.115539

Wei, H., He, Y., Li, Q., Liu, Z., and Wang, H. (2007). Summer Hypoxia Adjacent to the Changjiang Estuary. *J. Mar. Syst.* 67, 292–303. doi: 10.1016/j.jmarsys.2006.04.014

Yin, G., Hou, L., Liu, M., Liu, Z., and Gardner, W. S. (2014). A Novel Membrane Inlet Mass Spectrometer Method to Measure (1)(5)NH4(4)(+) for Isotope-Enrichment Experiments in Aquatic Ecosystems. *Environ. Sci. Technol.* 48, 9555–9562. doi: 10.1021/es501261s

Yoon, J.-E., Lim, J.-H., Son, S., Youn, S.-H., Oh, H.-J., Hwang, J.-D., et al. (2019). Assessment of Satellite-Based Chlorophyll-A Algorithms in Eutrophic Korean Coastal Waters: Jinhae Bay Case Study. *Front. Mar. Sci.* 6. doi: 10.3389/fmars.2019.00359